



A comparative study of acidic, basic, and reactive dyes adsorption from aqueous solution onto kaolin adsorbent: Effect of operating parameters, isotherms, kinetics, and thermodynamics

Tadele Assefa Aragaw*, Adugna Nigatu Alene

Faculty of Chemical and Food Engineering, Bahir Dar Institute of Technology, Bahir Dar University, Bahir Dar, Ethiopia

ARTICLE INFO

Article history:

Received 11 December 2021

Received in revised form

17 January 2022

Accepted 17 January 2022

Keywords:

Beneficiated adsorbent

Different class dyes

Adsorption

Operational parameters

Removal efficiency

Electrostatic interaction

ABSTRACT

Various studies were reported for the evaluation of the adsorption performance of kaolin clay using single dye types. This paper aimed to evaluate the comparative adsorption capacity of prepared adsorbents from Ethiopian kaolin for different dye types (Basic Yellow 28 (BY 28), Congo Red (CR), and Reactive Red 120 (RR 120)). Because different dye classes may have a significant impact on the removal efficiency by the prepared adsorbent. Moreover, we intended to investigate the interaction effect of adsorbent-sorbate in the adsorption phenomenon for the three different class dyes. The adsorbents from kaolin clay were prepared via mechanical treatment, beneficiation, and calcination (700 °C). The effect of operating parameters (pH, adsorbent dose, contact time, dye concentration, and adsorption temperature) was evaluated, before and after adsorption of the adsorbents were characterized using FTIR spectroscopy. Furthermore, adsorption isotherm, kinetic models, and the thermodynamic processes in the adsorption phenomenon were computed. The percentage removal efficiency of dyes was recorded as 92.08%, 88.63%, and 73.33% for BY 28, CR, and RR 120 dyes, respectively at the experimental condition: adsorbent dosage = 1 g/100 mL, solution pH = 9 (BY 28), and pH = 3 (CR, and RR 120), contact time = 60 min, initial dyes concentrations = 20 mg/L, and temperature = 30 °C. The adsorption of adsorbates onto kaolin adsorbents was well fitted with pseudo-second-order kinetics and Langmuir isotherm models. The thermodynamic parameters indicate that the adsorption process is spontaneous and exothermic for all dyes. The comparative percentage removal of, with the same operational parameters and kaolin adsorbent, was recorded as BY 28 > CR > RR120 resulting from their surface charge and molecular size/structure dyes properties. We confirm that the adsorption at each operational parameter and peak intensity of FTIR spectra, before and after adsorption, revealed that the different dye types have varied removal efficiency onto the prepared kaolin adsorbent. This is due to that being dominantly influenced by the electrostatic interaction and steric effects at the surface of the sorbent and sorbate characteristics. We deduced that the kaolin clay used as an adsorbent is highly dependent on the dye types and their featured characteristics.

© 2022 The Authors. Publishing services by Elsevier B.V. on behalf of KeAi Communications Co. Ltd. This is an open access article under the CC BY-NC-ND license (<http://creativecommons.org/licenses/by-nc-nd/4.0/>).

1. Introduction

Nowadays, in addition to eutrophication, responsible nutrients such as phosphate and nitrate [1], contaminants from industrial wastewater effluents containing dyes are a serious problem to the environment and water bodies due to their toxicity. Dyes are

engaged in many industries like textile, tannery, food, and chemical for different purposes. Wastewater that contains the dyes can harm the human being and aquatic life because many dyes are toxic and non-biodegradable as well as they are the main causes of mutagenesis, carcinogenesis, and respiratory toxicity [2].

Therefore, treatment of wastewater containing dye before discharges to the environment is critical because their color, even at extremely low quantities (less than 1 mg/L), has a significant impact on water quality [3]. Dyes can be removed from wastewater by different methods like filtration [4], flotation [5], adsorption [6],

* Corresponding author.

E-mail address: taaad82@gmail.com (T.A. Aragaw).

Peer review under responsibility of KeAi Communications Co., Ltd.

and photocatalysis [7]. From these methods, many types of research were reported alternative adsorbents as effective, cheap, and promising for eliminating organic contaminants such as dyes [8], and nutrients such as phosphate [9] from wastewater. Kaolin is a clay type that is used as an adsorbent to remove pollutants from wastewater due to its availability, non-toxicity, and low cost [10]. Additionally, it is effective to treat dye-contaminated wastewater [11].

By saying the low-cost sorbents, its inclusivity ascertains different dimensions, such as the sustainable resource availability of different materials, the simple and least cost preparation methods without affecting the sorbent quality, their regeneration potentials, and the capability of producing them [12]. Based on the first criteria (sustainable resource availability), most of the developing countries, in this study case, Ethiopia's natural resources have not been exploited more to date. One of the best examples of these available materials, the kaolin clay can be considered as a suitable and sustainable resource for the potential adsorbent. The geological survey office of Ethiopia reported (unpublished document) that many regional places surveyed and found a huge reservoir of kaolin clay. However, negligibly utilized as a commercial raw material for different applications. As a result, the present study can address for the county government to use the available resources for wastewater treatment by examining their efficiency.

Many researchers used modified and unmodified kaolin as an adsorbent to remove different dyes, such as Congo red [13–15], basic yellow 28 [16], basic yellow 2 [17], reactive red 120 [18–20], basic red 46 [21], direct yellow 50 [22], methylene blue [15,23], malachite green [24], crystal violet [15,25], natural annatto [26], violet 5R and acidic blue 25 [27], methyl violet 10B [28], amino black [29], cyanide [30], basic blue 41 [31], Methyl Orange [32], auramin, azins and rhodamine B [13], brilliant green [31,33,34], coriocide Bordeaux 3B, derma blue R67, and coriocide brown 3J [2] from aqueous solution. The removal capacity and/or percentage removal for each type of dye onto the kaolin adsorbent is different. This difference is due to the effects of dye types (acidic, basic, or reactive dye) that have surface interactions with the adsorbent surface due to their anionic, cationic, and neutral nature. Also, the modification of the untreated kaolin (raw) adsorbents is an important factor for the removal efficiency.

The characteristics of a potential Ethiopian kaolin adsorbent in terms of thermal, functional groups, crystallinity, surface morphology with its elemental distribution, and oxide compositions were explained from our previous study [16,35]. Based on the characteristics of Ethiopian kaolin, this paper aimed to evaluate the adsorption capacity of wet treated adsorbent from Ethiopian kaolinite clay as comparative and cost-effective sorbent for different dye types: Basic Yellow 28 (BY 28), Congo Red (CR), and Reactive Red 120 (RR 120). The basic batch experimental conditions such as solution pH, adsorbent dose, contact time, initial dye concentration, and adsorption temperature were conducted and evaluated. Moreover, the structural and/or molecular weight, arisen due to different dye classes, effects for the prepared adsorbents. Furthermore, adsorption isotherm, kinetic models, and the thermodynamic processes in the adsorption phenomenon were computed.

2. Material and methods

2.1. Kaolin sample collection and adsorbent preparation

Beneficiated kaolin adsorbents were prepared according to the techniques presented by Aragaw and Angerasa [16,35]. Kaolinite samples were collected from Debre Tabor town, Ethiopia. Drying ovens, mills, crushers, and sieves were employed for adsorbents

preparation. Moreover, electronic balance, pH meter, hot plate, magnetic stirrer, pipette, measuring cylinder, test tubes, and Whatman filter paper were used for batch adsorption experiments. One molarity (1 M) Sodium hydroxide and Hydrochloric acid solutions were used for solution pH adjustment. In our previous work, we found and confirmed that beneficiated kaolin adsorbents out of the calcined and raw kaolin were recorded as the highest removal efficiency [16]. Therefore, a beneficiated kaolin adsorbent was selected in this paper for further study as a potential adsorbent.

2.2. Standard calibration curve preparation

Basic yellow 28 (BY28), Congo red (CR) called Direct Red 28, and reactive red 120 (RR120) dyes, as model dye pollutants, were collected from Bahir Dar Textile Share Company, Ethiopia, and used without further purification. The chemical formula, molecular weight, Lambda max (λ_{\max}), and molecular structures of the dyes have been presented in Fig. 1. BY 28 is a cationic dye whereas CR and RR 120 are anionic dyes. The physical state of the three dyes was powdered solids. 0.5 g of powder dye taken from each type and well mixed in 1 L of distilled water separately, to prepare dye solution. The λ_{\max} is obtained by scanning the dye solutions, 50 mg/L, using a UV/VIS spectrometer (Lambda 35 Ferkin Elmer), and obtained as 438 nm, 540 nm, and 495 nm for BY 28, RR 120, and CR dye, respectively. The known dye concentrations were prepared and their absorbency values were measured for each dye solution. Linear calibration curves with corresponding squared correlation coefficients (R^2) were computed from absorbency values versus their respective concentration of the solution Fig. 2. The linear calibration curve of this data was served as the basis for determining the final dye concentration.

2.3. Design of experiments

For each batch experiment, the 250 mL Erlenmeyer flask was employed with the distilled water. The amount of initial dye concentration (100 mL) and measured prepared adsorbents was added to the 250 mL Erlenmeyer flask and stirred at 200 rpm with a magnetic stirrer. The dye solutions pH values were adjusted with 1 M NaOH/HCl solutions. The basic operating parameters of the adsorption experiments were optimized with contact time ranging from 20 to 100 min at a 20 min interval, initial dye concentration of 20, 40, and 60 mg/L, at a temperature of 30 °C, 50 °C, and 70 °C. The solution pH was employed at the acidic media (pH 3), neutral media (pH 7), and basic media (pH 9). The adsorbent dose was taken in a range from 0.1 to 2.0 g at a 0.5 g interval. At the predetermined batch experiments, a small amount of solution was withdrawn and centrifuged for absorbance measurement. Thereafter, the residual dye concentration was calculated from the calibration curve of each dye value.

The removal efficiency of the dye was calculated by Eq. (1) [36]. The equilibrium concentration (load) of adsorbate in the solid phase (q_e , mg/g) and concentration (load) of adsorbate in the solid phase at any time (q_t , mg/g) were determined by Eqs. (2) and (3), respectively, [37].

$$\text{Dye removal efficiency (\%)} = \frac{C_0 - C_t}{C_0} \times 100 \quad (1)$$

$$q_e \left(\frac{\text{mg}}{\text{g}} \right) = \frac{(C_0 - C_t) \cdot V}{m} \quad (2)$$

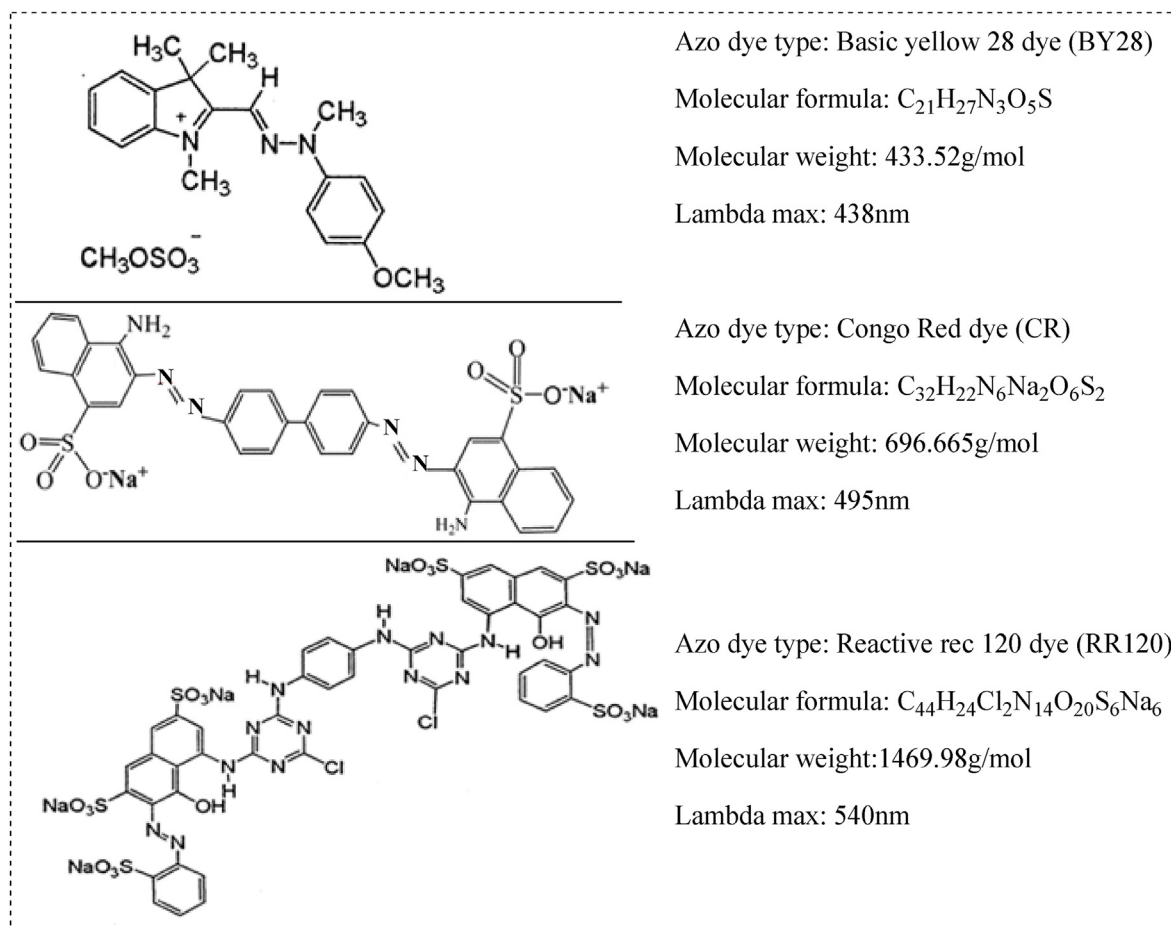


Fig. 1. Description of (a) BY 28, (b) CR and (c) RR 120 dyes.

$$q_t \left(\frac{\text{mg}}{\text{g}} \right) = \frac{(C_0 - C_t) * V}{m} \quad (3)$$

where, C₀: initial dye concentration (mg/L), C_e: solute (dye) concentration in liquid phase at equilibrium (mg/L), C_t: dye concentration in liquid phase at any time (mg/L), m: amount of adsorbent (g) and V: volume of solution (L).

2.4. Dye solutions stabilities determination with UV/VIS scanning

The stability of BY 28, CR, and RR 120 dye solutions was determined via a wavelength scan to determine the disappearance of the λ_{max} using a UV–Vis spectrophotometer [38]. The dye solutions absorption spectra were recorded before and after adsorption at various initial concentrations (20, 40, and 60 mg/L of 100 mL), pH = 9 (BY 28) and pH = 3 (CR, RR 120), adsorbent dose (1 g), temperature (30 °C). The scanning was conducted samples at a time (0 min, before adsorption and 60 min, after adsorption).

2.5. FTIR analysis of kaolin adsorbent

Fourier transform infrared, FTIR (JASCO-6600) spectrophotometer was used to analyze the surface, functional groups of beneficiated kaolin adsorbent, before and after dye adsorption (dye loaded adsorbents) with a range of 4000 to 400 cm⁻¹. Pellet formation was performed with standard KBr reagent; powdered uniformly using mortar and pestle at the sample to KBr ratio of 1:100.

3. Result and discussion

3.1. Calibration curve and residual dye stability determination

The calibration curves have been plotted for each standard solution of BY 28, CR, and RR 120 dyes (Fig. 2) to determine the final concentration on each batch experiment. The linear regression curve values with its extinction coefficients were obtained as BY 28 (Y = 0.0237x + 0.01682, R² = 0.99952), CR (Y = 0.0115x + 0.03677, R² = 0.99585), and RR 120 (Y = 0.00947 + 0.00183, R² = 0.99982). This suggested that the standard curve allows forwarding for each batch experiment due to the correlation coefficient values being in the scientifically recommended ranges (R² > 0.99).

The known concentrations (20, 40, and 60 mg/L) of BY 28, CR, and RR 120 before and after adsorption were scanned, as shown in Fig. 3(a–c), to confirm the decolorization at their respective lambda max. The scans were recorded at the scan range from 300 to 600 nm, 400–600 nm, and 400–650 nm for BY 28, CR, and RR 120, respectively. As can be observed, in the initial dye (before adsorption), the peaks of absorbance at their lambda max were high in concentration and colored. However, the peaks at their lambda max were significantly reduced and even completely disappeared, suggesting that the colors were removed by the prepared adsorbent. Comparatively, the lambda max peaks for BY 28 and CR were completely disappeared even at their high dye concentration (60 mg/L). This suggested that the prepared kaolin adsorbent is efficient for the basic (cationic) and acidic (anionic) dyes due to the adsorbent surface charge nature (positively charged at the alumina

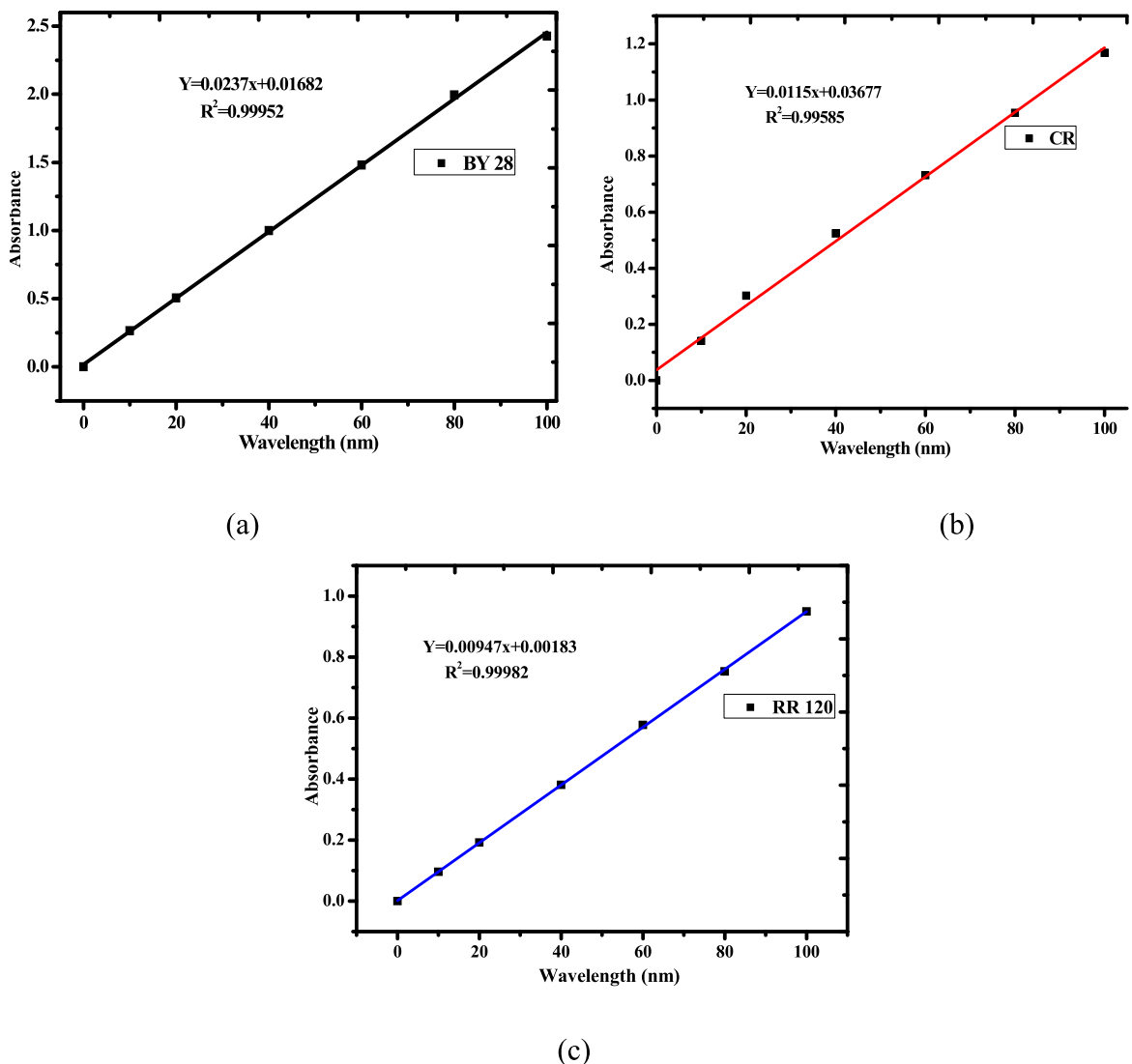


Fig. 2. Calibration curve (10–100 mg/L) for (a) BY 28, (b) CR and (c) RR 120 dyes.

face and negatively charged at the silica face) capable of the electron affinity of the ions in the solution by the electrostatic interaction. However, the RR 120 lambda max peak was not disappeared even at the low concentration (20 mg/L). This is due to the reactive dyes having lower ionic solution features as compared with acidic and basic dyes resulted in ions of dyes unable to attach to the adsorbent surface [39]. Thus, it can be deduced that the kaolin clay used as an adsorbent is highly dependent on the dye types and characteristics which the present study is aimed.

3.2. Characterization of kaolin adsorbent

The thermal, surface morphology with elemental distribution, functional groups, crystalline structures, and oxide composition of adsorbents from Ethiopian kaolinite was characterized using TGA-DSC, SEM/EDS, FTIR, XRD, and XRF, respectively in our previously published papers [16,35]. The thermal property via thermogravimetric analysis of sampled Ethiopian kaolin was determined and confirmed that metakaolinization occurred up to 700 °C with the loss of ignition (LOI) 2.6%. The surface morphology and porosity of wet treated Ethiopian kaolin adsorbent have been determined using scanning electron microscopy (SEM) and confirmed that

essentially unstructured, irregular in shape, and porous on the surface with uneven edges, with the high surface elemental distribution of aluminum, silicon, and oxygen. Also, the oxide composition of the largest proportion of the beneficiated kaolin adsorbent has been recorded as SiO₂ (61.13%) and Al₂O₃ (20.97%) with the SiO₂/Al₂O₃ molar ratio in the pure kaolinite standard range, is 2.92 tells that this kaolin clay can be classified into siliceous one (kaolinite) [40]. Moreover, the diffraction patterns that have been dealt with multiple reflections found mainly at $2\theta = 16^\circ, 32^\circ, 49^\circ$ which are a characteristic diffraction pattern of kaolinite clay, suggesting that sampled kaolin has a crystalline structure and is an ideal kaolin clay with a high kaolinite content.

3.3. FTIR analysis before and after adsorption

The surface characteristics (before and after adsorption) in terms of functional groups of kaolin adsorbent and adsorbate loaded powder (adsorbent-BY 28, adsorbent –CR, and adsorbent-RR120) in the range of 4000–400 cm⁻¹ were analyzed as shown in Fig. 4. Also, each spectral peak with the corresponding assignment functional groups is presented as shown in Table 1. The prepared adsorbent showed that the small peak at 3616 cm⁻¹ is

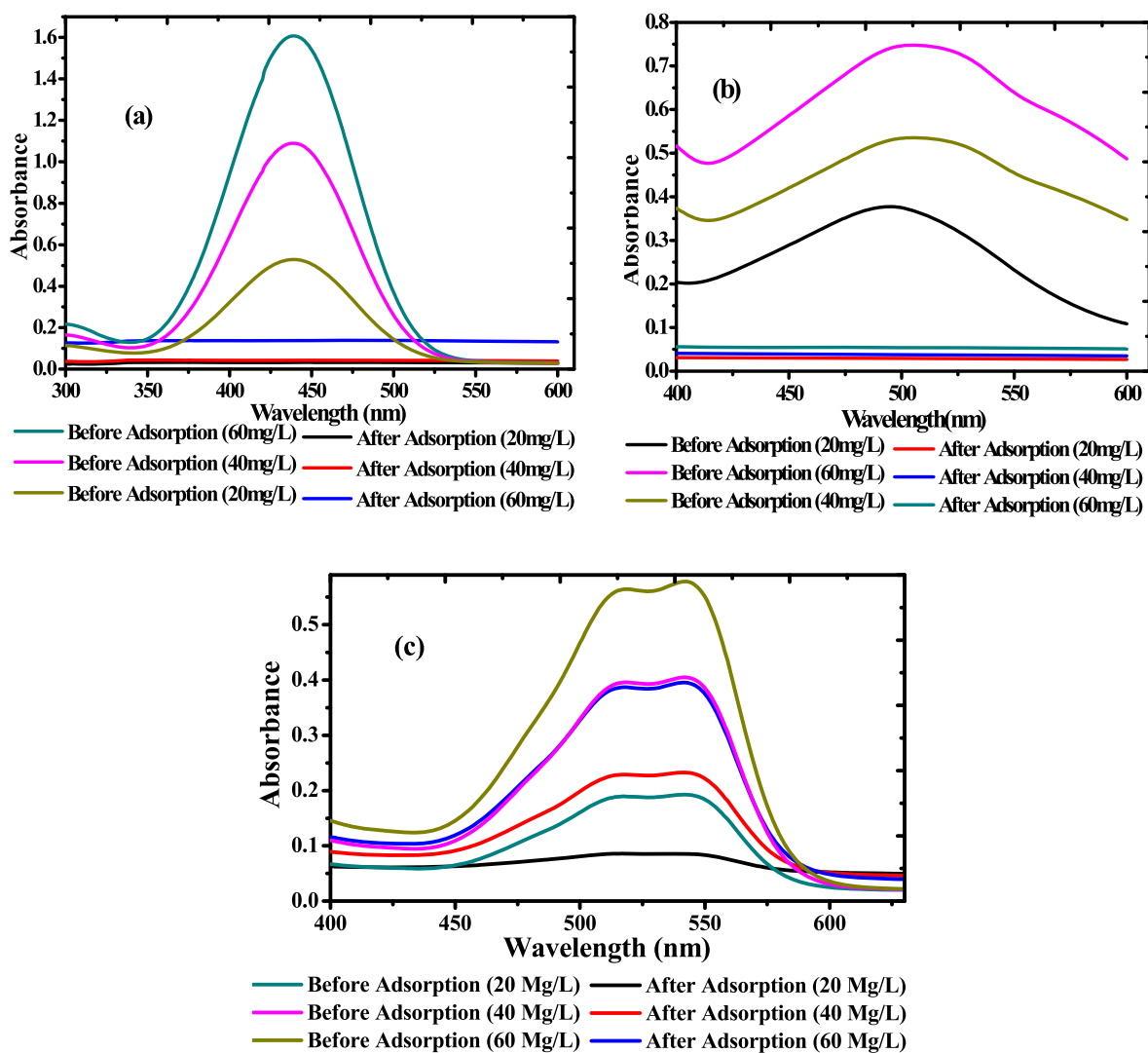


Fig. 3. UV/Vis scanned spectra of before and after adsorption of dye solution (20–60 mg/L) for stability determination for (a) BY 28, (b) CR, and (c) RR 120 dyes.

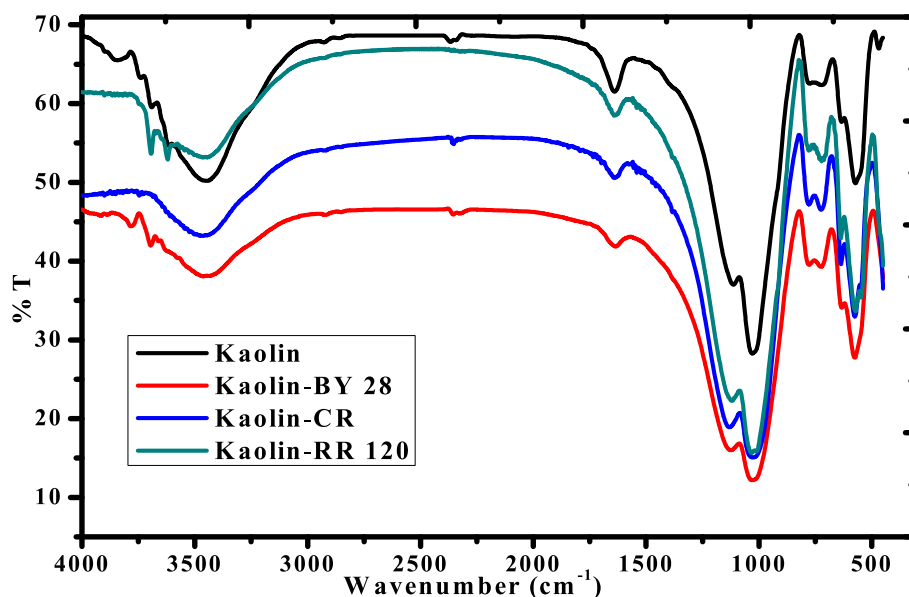


Fig. 4. FTIR spectral analysis of adsorbents and adsorbate-loaded dyes (BY 28, CR, and RR 120).

Table 1

FTIR spectral bands of the adsorbents before adsorption, and adsorbent-BY 28, adsorbent-CR, and adsorbent-RR120 with the corresponding functional group assignments.

Sample	Adsorbent	Adsorbent-BY 28	Adsorbent-CR	Adsorbent-RR 120	Assignments	References
Wavenumber (cm ⁻¹)	3616	3695	3626	3620	-Al-OH, Si-OH stretching	[42,48]
	3456	3439	3462	3450	-O-H stretching (H-O-H)	[49]
	1637	1637	1642	1637	-O-H deformation (H-O-H)	[49]
	1117	1123	1128	1123	Si-O-, Al-O-stretching	[50]
	1031	1025	1024	1031	Si-O-, Al-O-stretching	[49]
	776	776	776	782	Si-O, Al-O	[50]
	568	574	574	574	-Al-O-Si-	[27]
	467	450	450	450	-Si-O-Si-	[27]

attributed to the internal surface of hydroxyl groups (–O–H) in the Al–OH, and Si–OH that can form the bond between octahedral and tetrahedral sheet in the kaolinite clay [41]. The characteristic peaks at 3456 and 1637 cm⁻¹ are corresponding to –O–H stretching vibrations and deformation band of water molecules, respectively [42]. Absorption peaks at 1117, 1031, and 776 cm⁻¹ are supposed to be silicon oxide (Si–O), and aluminum oxide (Al–O) stretching vibrations indicate that silicon oxide is contained dominantly in the studied kaolin [43]. The peaks around 568 and 467 cm⁻¹ correspond with Si–O–Al and Si–O–Si bending vibrations, respectively [44].

The characteristic surface absorption peaks of kaolin adsorbent and adsorbent-loaded dyes (BY 28, CR, and RR 120) were observed as they have no significant percentage transmittance variation resulting in the basic structure remaining unchanged through adsorbent-dyes interactions [45]. But, slight shifts/changes from their positions and the intensity of peaks were observed because of adsorbed dye molecule quantities that can affect the percentage transmittance. These slight position shifts can be related to the involvement of surface properties, adsorbent interaction to surface functional groups, of the dyes (BY 28, CR, and RR 120 dyes). This interaction could be through electrostatic or weak van der Waals forces due to the dyes having ionic features in solution and the physical interaction of dyes-adsorbents at the surfaces [46,47]. Moreover, the intensity of peak variation or the bending shape before and after the adsorption of dyes on the adsorbent was observed as an important indicator of the adsorbate loads. Thus, before the adsorption process, the percentage transmittance of the bending shape of the adsorbent was maximum. This shows that the surface of the adsorbent was not occupied by dye ions. However, the percentage transmittance of bending shape was minimum for the adsorbent after adsorption suggested that the surface of the adsorbent was occupied with dyes that can block the infrared signals. The bending shape for BY 28 loaded adsorbent was the lowest as compared with CR and RR 120 loaded adsorbents suggested that BY 28 dye ion was most attached to the surface of the prepared adsorbents.

3.4. Effects of operating conditions

3.4.1. Effect of solution pH

The adsorption process is strongly affected by changes in solution pH. The effect of the pH of a solution usually depends on the electrostatic interaction with the ions' adsorption surface present in the reaction mixture. The pH of the solution can affect both the solution chemistry and surface binding sites of the adsorbents [10]. In the present study, the pH values of the solution were adjusted as acidic, neutral, and basic media at 3, 7, and 9, respectively for all batch adsorption experiments as shown in Fig. 5. The maximum percentage of dye removed for basic yellow 28 (BY 28) dye was obtained at basic media (pH = 9). However, for congo red and reactive red dye were at acidic media (pH = 3) suggested that as the

pH value increases, the surface charge of the particles becomes more negative. This explains why the adsorption of basic dyes, BY 28 molecules was better adsorbed at higher pH due to having cation in the solution. However, congo red and reactive red dye molecules' adsorption were favored at the low pH values is due to having the anions in the solution.

Usually, at low pH, the percentage removal of anionic dye from solution is increased due to the electrostatic attraction between the anionic dyes and the positive surface charge of the silica tetrahedral face of kaolinite but is negatively charged at pH > 4, whereas the alumina octahedral face of kaolinite is positively charged at pH < 6 [51]. Thus, there is an electrostatic attraction between the negatively surface charge of the kaolinite adsorbent and ions of dyes in the high pH (basic) solution, causing a decrease in the percentage removal of anionic dyes. Whereas, when the solution has high pH the adsorption capacity and removal of basic dyes have been increased because of the cationic charges dye ensured that they are attracted by the negative surface charge of the kaolinite adsorbent. Hence, it can be assured that there are electrostatic attractions between adsorbents and sorbates in the solution.

The adsorption process is basically due to the coulombic attraction between the negatively charged surface and the positive charge of the dye ions due to the alumina octahedral face of kaolinite is mostly negatively charged surfaces at pH > 8. This is also due to the percentage composition of the kaolinite surface is riched in silica with a small percentage of alumina. Because of this, its surface charge is likely to be Si–OH₂⁺, Al–OH₂⁺, and Si–O⁻, Al–O⁻ in acidic and alkaline medium, respectively [52]. The presence of H⁺ ions in the acidic media can make the lower removal efficiency of the kaolinite adsorbent due to the destabilization of cationic dye with excess proton resulted in the electrostatic repulsion of the active adsorption sites. The same result is obtained by Ref. [42] the basic yellow 28 is more removed at basic media onto the surface of smectite-rich natural clays.

Furthermore, the kaolinite particle interactions may occur between the silica face–alumina face interaction makes kaolinite particle aggregation at low acidic and medium acidic pH values. This may disturb the active sites of the adsorbent by the shear yield stress resulting in the low percentage removal for the basic type of dyes [53]. All the three compartments of the kaolinite: surface charge densities of the silica and alumina sheet, and the edge in between the sheet particle interactions are important influencing factors thereby hindering the mechanical features of kaolinite suspensions.

3.4.2. Effect of adsorbent dose

The removal of BY 28, CR, and RR 120 impacted by the adsorbent dose was determined, as shown Fig. 6, in the batch mode experiment with adsorbent dosage range (0.1–2 g)/100 mL with the 0.5 g interval at a pH of 9 (for BY 28) and pH of 3 (for CR and RR 120), initial dye concentration of 20, 40 and 60 mg/L, contact time of 60 min, and at the adsorption temperature of 30 °C. The percentage

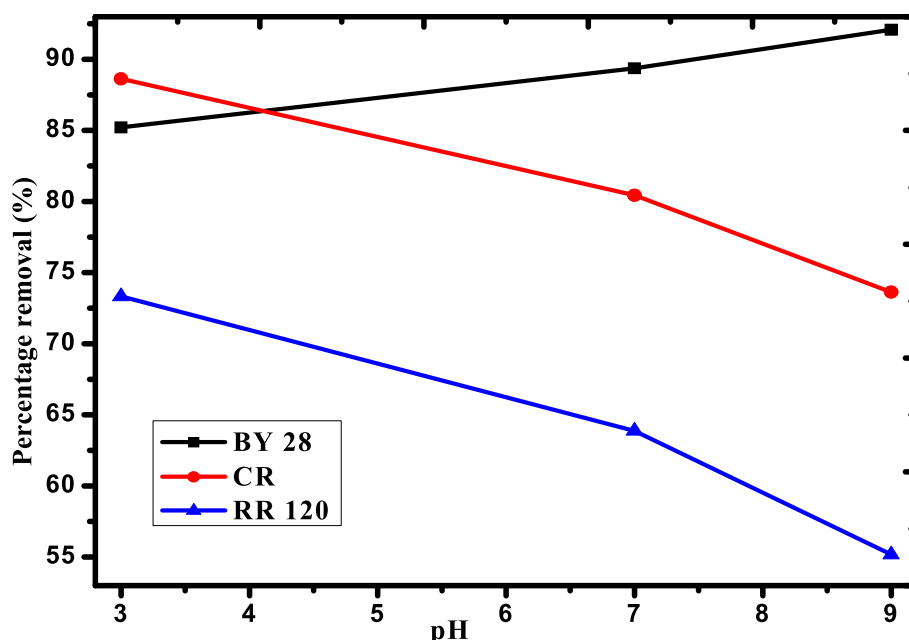


Fig. 5. Effect of solution pH on the percentage removal of BY 28, CR, and RR 120 dyes onto prepared adsorbent (adsorbent dose = 1 g/100 mL, contact time = 60 min, initial dye concentration = 20 mg/L, temperature = 30 °C, and agitation speed = 200 rpm).

removal of all types of dyes is increased with increasing adsorbent dosage up to 1 g/100 mL and reached 92.08%, 88.63%, and 73.33% for BY 28, CR, and RR 120, respectively. Increasing removal efficiency with increasing adsorbent dosage is due to the availability of more active binding sites and greater sorption surface area [54]. However, the percentage removal of dyes becomes constant beyond 1 g/100 mL for all dyes concentration suggests that the splitting effect of the concentration gradient between adsorbent and dye molecules is optimal at 1 g adsorbent. The adsorption efficiency of different dyes (BY 28, CR, and RR120) as a function of kaolin adsorbent is different due to the differences in chemical structures, properties, molecular size, and adsorbent-dye interactions [54].

3.4.3. Effect of contact time

The adsorptive percentage removal of dyes onto kaolin adsorbent was examined, as shown in Fig. 7, by varying the mixing time ranging from 20 to 100 min with 20 min intervals at an initial dye concentration of 20, 40, and 60 mg/L, adsorbent dose of 1 g/100 mL, solution pH of 9 (for BY 28), and solution pH of 3 (for CR and RR120), and at the adsorption temperature of 30 °C. The adsorption of all types of dyes for the concentration of 20, 40, and 60 mg/L is increased with increasing the contact time up to 60 min. This indicates that the adsorbents' active sites/surfaces were vacant/unoccupied with enough concentration of dyes in the solution [47]. However, after 60 min contact time (optimal), the removal efficiency almost remains constant up to 100 min suggested that the lack of availability of active sites on the adsorbent surface in that the adsorbate tends to desorb into the liquid phase [55]. Thus, it can be concluded that the optimal contact time for the prepared dye solutions onto the prepared adsorbent is 60 min at the given experimental conditions.

3.4.4. Effect of initial dye concentration

The effect of initial dye concentrations was examined in the range of 20–60 mg/L at 20 mg/L intervals for BY 28, CR, and RR 120 dyes. As can be seen from Fig. 8, the percentage removal of dyes is

decreased as the initial dye concentration increased from 20 to 60 mg/L with the maximum removal efficiency as 92.08%, 88.63%, and 73.33% for BY 28, CR, and RR 120 dyes, respectively. These percentage removals of dyes were achieved at the experimental conditions of initial dye concentration = 20 mg/L, at a contact time = 60 min, adsorbent dose = 1 g/100 mL, and temperature = 30 °C. The maximum percentage removal efficiencies of BY 28 and RR 120 dyes were the highest and lowest, respectively. This is due to the chemical and physical characteristics of each type of dye, which have varied interaction features on the prepared adsorbent. Thus, it was confirmed that unoccupied active sites exist on the adsorbent surface even at low concentrations due to the low interaction capacity of the adsorbate onto the adsorbent resulted in the desorption of dyes into the liquid phase made the solution shed.

As observed from Fig. 8, the adsorption sites were available for dye adsorption at the low initial dye concentration, especially for RR 120 dye due to some weak electrostatic interaction. Additionally, the obtained result confirmed that for a given mass of adsorbent material; the amount of dye that can be adsorbed is fixed. The same results were reported for adsorption of Basic Red 46 (BR46) and Reactive Red 196 (RR196) onto sawdust adsorbent [56]. A similar result was reported on the adsorption of acidic dye type, called congo red (common name: direct red 28) onto adsorbents prepared from electro-coagulated sludges having the surface charge feature [57].

3.4.5. Effect of adsorption temperature

To determine the effect of adsorption temperature in the adsorption phenomenon emerged by the prepared adsorbents for, BY 28, CR and RR 120 dye were conducted, as shown in Fig. 9, at a temperature of 30, 50, 70 °C at an initial dye concentration of 20 mg/L, adsorbent dose of 1 g/100 mL, contact time of 60 min, and pH of 9 (for BY 28) and pH = 3 (for CR and RR 120). The removal efficiency for all dyes is decreased as the adsorption temperature increases from 30 to 70 °C. The results suggested that the adsorption of those dyes onto prepared adsorbent was favorable at low adsorption temperature and exothermic nature adsorption

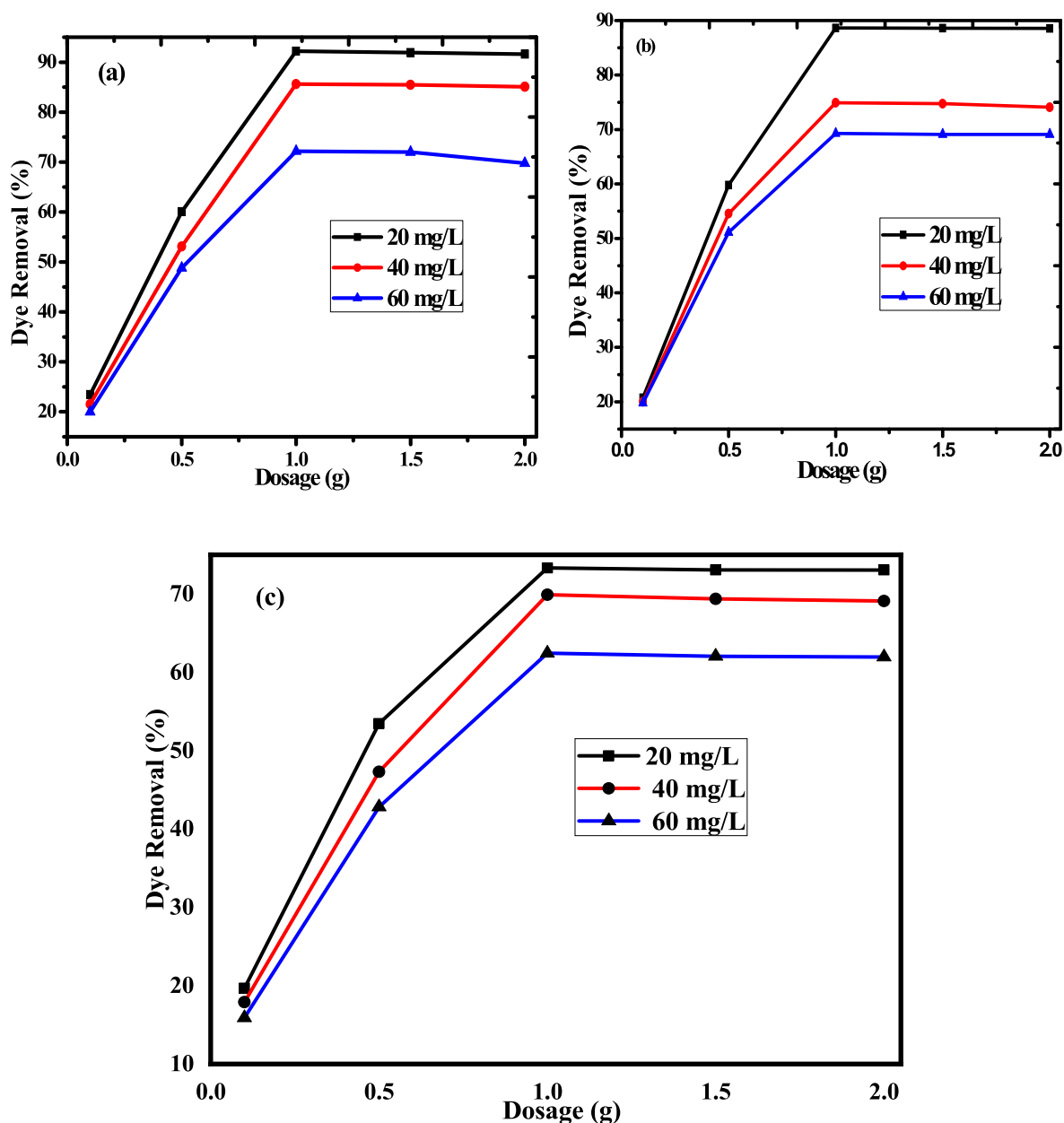


Fig. 6. Effect of adsorbent dose on the percentage removal of (a) BY 28, (b) CR, and (c) R 120 dyes in solution onto prepared adsorbent (solution pH = 9 (for BY 28) and pH = 3 (for CR, RR 120), contact time = 60 min, initial dye concentration = 20 mg/L, temperature = 30 °C, and agitation speed = 200 rpm).

phenomenons to occur [58]. This means that the adsorbent active sites become expanded and the dye ions and/or molecules in the solution tend to release back to the liquid phases from the adsorbent surface at high temperatures [59]. Comparatively, the BY 28 dye has the highest removal efficiency amongst CR and RR 120 suggested that they have high electrostatic attraction at high adsorption temperatures [16].

3.5. Adsorption kinetics, thermodynamic, and isotherm

3.5.1. Kinetic models

To determine the rate of adsorption mechanism of BY 28, CR, and RR 120 dyes onto the prepared adsorbents, two commonly used adsorption kinetic models (the pseudo-first-order and pseudo-second-order), as governed by Eq. (4) and Eq. (5), were employed to explain the experimental results [45,55].

$$\log(q_e - q_t) = \log q_e - \frac{k_1}{2.303} t \quad (4)$$

$$\frac{t}{q_t} = \frac{1}{k_2 q_e^2} + \frac{t}{q_e} \quad (5)$$

where, q_e and q_t are the amounts of adsorbate adsorbed at equilibrium (mg/g) and at any time t (mg/g), respectively. k_1 (min^{-1}) and k_2 ($\text{g.mg}^{-1}\text{min}^{-1}$) are the pseudo-first-order and pseudo-second-order rate constants, respectively. The kinetic parameters for each model (Table 2) were calculated by plotting graph $\log(q_e - q_t)$ vs. t and t/q_t vs. t , as shown in Fig. 10 and Fig. 11, for pseudo-first-order and pseudo-second-order, respectively.

To evaluate the most appropriate kinetic model fitting for the experimental data, the correlation coefficient (R^2) was computed

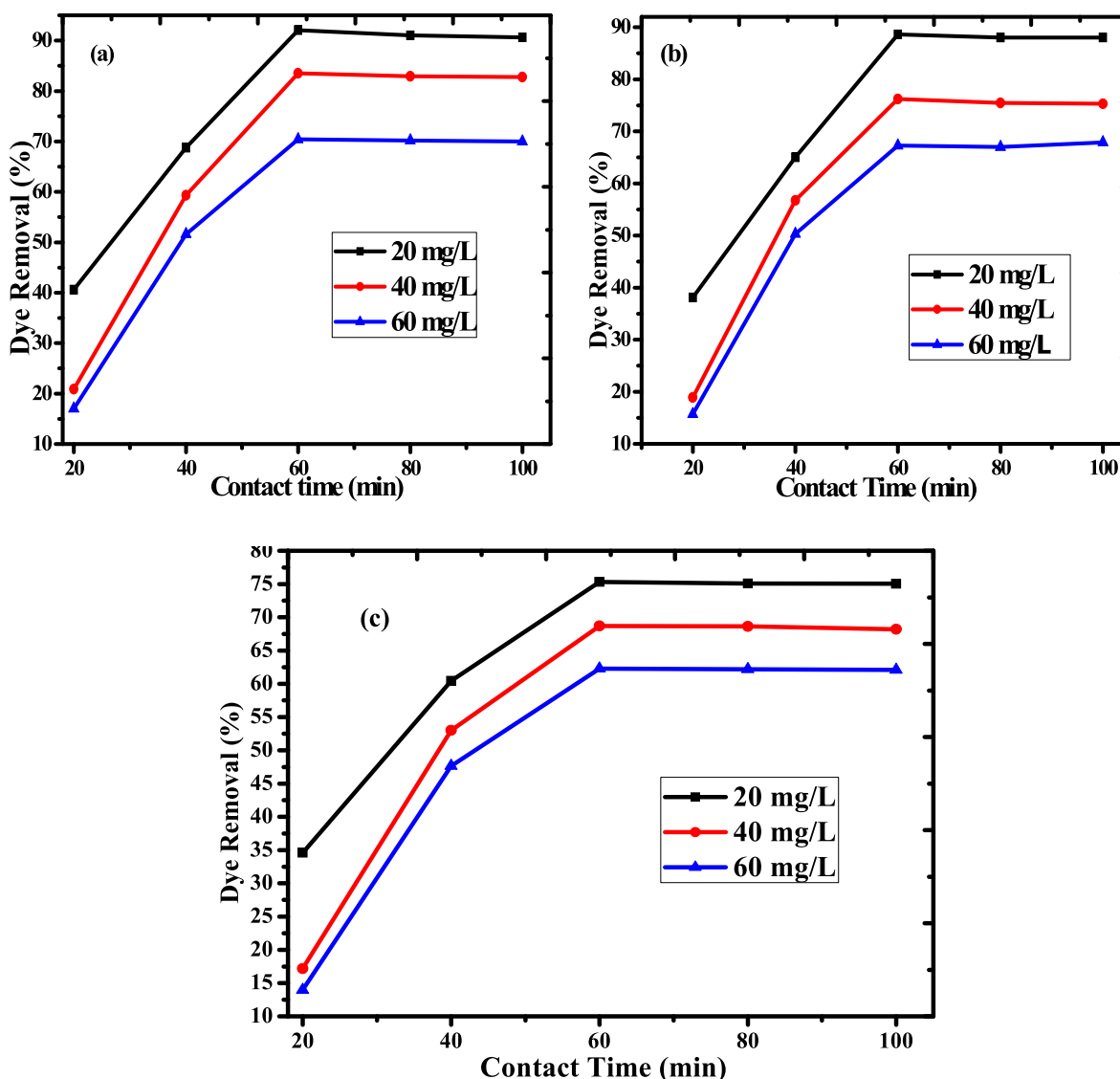


Fig. 7. Effect of contact time on the percentage removal of (a) BY 28, (b) CR, and (c) RR 120 dyes onto prepared adsorbent (adsorbent dose: 1g/100 mL, solution pH = 9 (for BY 28) and pH = 3 (for CR, RR 120), initial dye concentration: 20 mg/L, temperature = 30 °C, and agitation speed = 200 rpm).

and considered. A relatively higher R^2 value from the predicted model tells that their applicability in the adsorption processes. According to the kinetic parameters, it can be explained that the adsorption of BY 28, CR, and RR 120 by the kaolin adsorbent follows pseudo-second-order kinetic model due to the higher correlation coefficient ($R^2 > 0.91$) values, which is higher as compared with that of pseudo-first-order predicted model. Also, this can express and given information for the positively/negatively linear fitting equations, and in this study, more favor kinetic models (pseudo-second-order) are expressed in the positive fitting. From this, it can be concluded that the adsorption phenomenon is subject more to a chemical adsorption process in the solid-liquid phases for all types of dyes [57]. This tells that dye molecules/ions removal in the solution is favored the chemical interaction between the adsorbent and adsorbate in addition to the physical surface attachments.

3.5.2. Thermodynamic study

Standard free Gibbs energy change (ΔG°), standard enthalpy change (ΔH°), and standard entropy change (ΔS°) as thermodynamic parameters are important to study the thermodynamic

parameters in the adsorption phenomenon. The parameters were calculated with the governing equation, as presented from Eq. (6) to Eq. (9), to examine the spontaneity and feasibility behaviors in the adsorption process for kaolin adsorbents at different temperature profiles (303.15, 323.15, and 343.15 K) [60]. Moreover, the values of enthalpy change, ΔH° (KJ/mol) and entropy change, ΔS° (KJ/mol) were calculated from the slope ($-\Delta H^\circ/R$) and intercept ($\Delta S^\circ/R$) of the linear plot of $\ln(K_c)$ versus $1/T$ as shown in Fig. 12. Thermodynamic parameters for the adsorption of BY 28, CR, and RR 120 dyes onto beneficiated kaolin adsorbent are summarized in Table 3.

$$\Delta G^\circ = -RT \ln(K_c) = -2.303RT \log(K_c) \quad (6)$$

$$K_c = \frac{q_e}{C_e} \quad (7)$$

$$\Delta G^\circ = \Delta H^\circ - T\Delta S^\circ \quad (8)$$

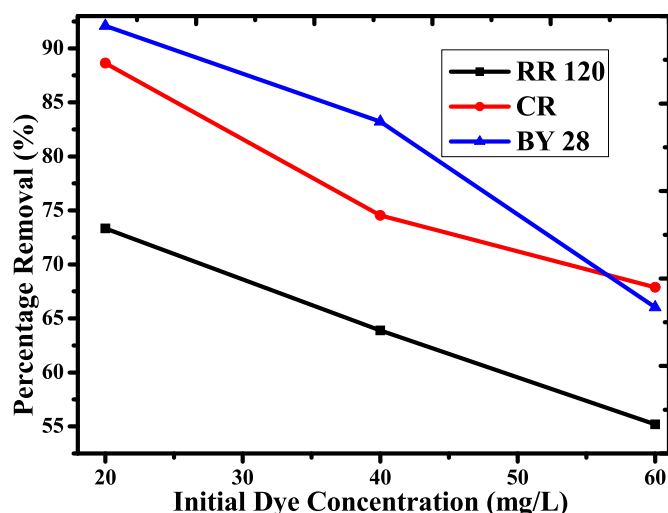


Fig. 8. Effect of initial dye concentration on the percentage removal of BY 28, CR, and RR 120 dyes onto prepared adsorbents (adsorbent dose: 1g/100 mL, contact time = 60 min, solution pH = 9 (for BY 28) and pH = 3 (for CR, RR 120), temperature = 30 °C, and agitation speed = 200 rpm).

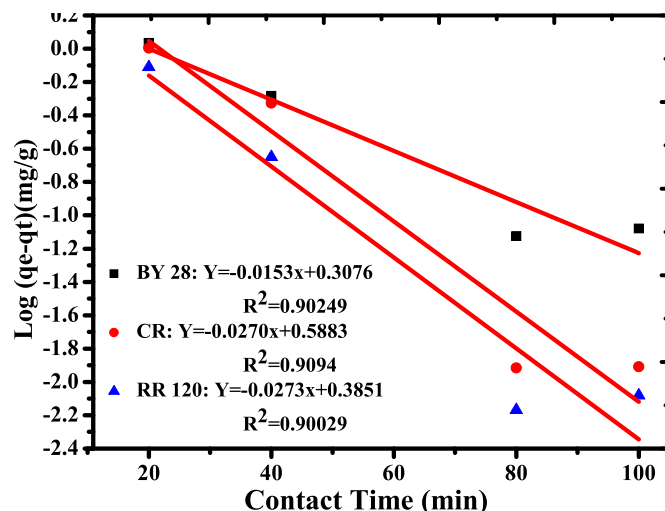


Fig. 10. Pseudo-first-order kinetic model for adsorption of BY 28, CR, and RR120 dyes onto kaolin adsorbent.

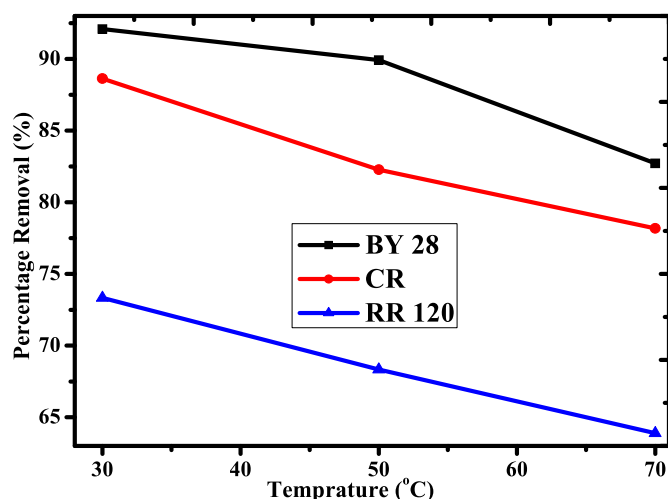


Fig. 9. Effect of adsorption temperature on the percentage removal of BY 28, CR, and RR 120 dyes onto prepared adsorbent (adsorbent dose: 1g/100 mL, contact time: 60 min, solution pH = 9 (for BY 28) and pH = 3 (for CR, RR 120), initial dye concentration = 20 mg/L, and agitation speed = 200 rpm).

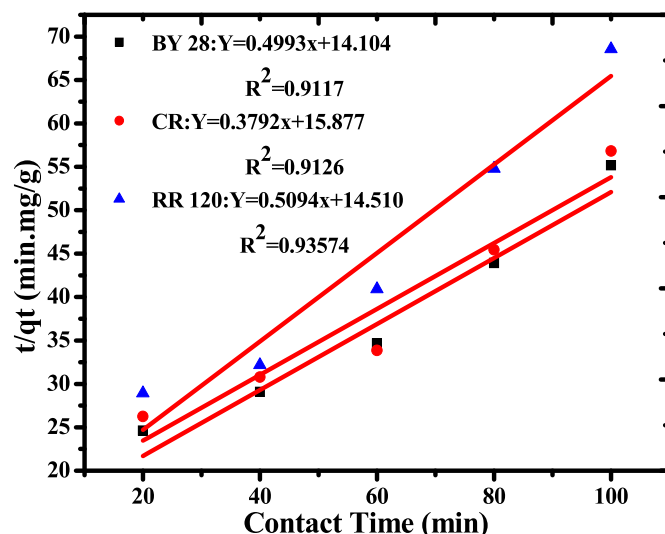


Fig. 11. Pseudo-second-order kinetic model for adsorption of BY 28, CR, and RR120 dyes onto kaolin adsorbent.

Table 2

Kinetic parameters for BY28, CR, and RR120 adsorption onto kaolin adsorbent.

Kinetics models	Parameters	BY28	CR	RR120
Pseudo-1st-order	q _e exp.(mg/g)	1.8958	1.7722	1.4667
	R ²	0.90249	0.9094	0.90029
	k ₁ (min ⁻¹)	0.0352	0.0621	0.0629
	q _e cal.(mg/g)	2.0305	3.8753	2.4272
Pseudo-2nd-order	R ²	0.9117	0.9126	0.93574
	q _e cal. (mg/g)	2.0029	2.6371	1.9631
	k ₂ (g/mg.min)	0.1767	0.0091	0.0179

$$\ln(K_c) = -\frac{\Delta H^\circ}{RT} + \frac{\Delta S^\circ}{R} \quad (9)$$

where, C_e (mg/L) is the equilibrium concentration of the solute, R is the universal gas constant (8.314 J/mol K), k_c is the equilibrium

constant, q_e (mg/L) is the amount of dye adsorbed on the adsorbent at equilibrium and T (K) is the temperature.

The negative ΔG° values at low temperature for BY 28 and CR indicate that the adsorption of dyes onto prepared adsorbents is spontaneous and thermodynamically favorable at minimum (negative) values [46,61]. However, at high temperature, the ΔG° values are positive and high in magnitude suggested that the adsorption process at the high temperature becomes non-spontaneous, and the removal efficiency of dyes are not efficient. Comparatively, BY 28 dye recorded as high ΔG° values indicating that the spontaneity is highest. The ΔG° values are positive for RR 120 dye even at the low temperature indicated that the adsorption process was non-spontaneous and the percentage removal by the prepared adsorbent is not efficient. This is also confirmed at the effect of the operating conditions. Moreover, the ΔG° values of BY28, CR, and RR120 increase (more positive) with an increased temperature, these values confirmed that the adsorption of dyes onto kaolin adsorbent has an effect on their spontaneity and thermodynamically favorability, show greater adsorption potential

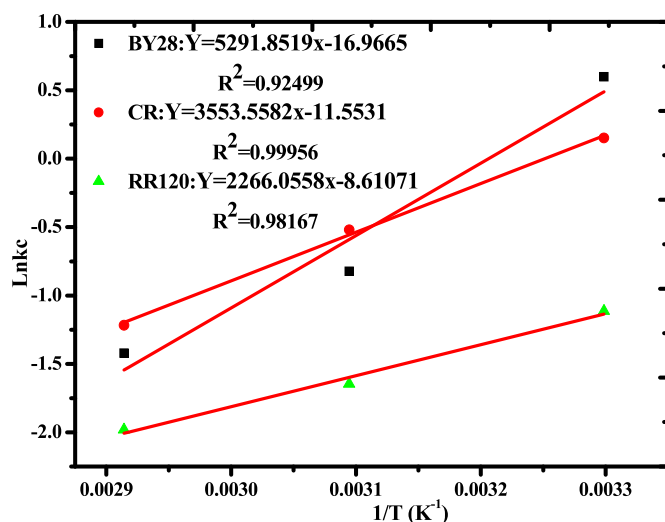


Fig. 12. Thermodynamic study for BY 28, CR, and RR 120 dyes onto kaolin adsorbent.

Table 3

Thermodynamic parameters for kaolin adsorbent upon BY28, CR, and RR120 dyes.

Dyes	Thermodynamic parameters					R ²
	ΔG° (kJ/mol)			ΔH° (kJ/mol)	ΔS° (kJ/mol)	
	Temperature (K)					
	303.15	323.15	343.15			
BY28	−1.243	1.576	4.396	−43.9965	−0.141	0.92499
CR	−0.382	1.396	3.472	−29.5445	−0.096	0.99560
RR120	2.805	4.424	5.653	−18.8399	−0.072	0.98167

at lower temperatures [62].

The negative values of ΔH° (−43.9965 kJ/mol) for BY 28, (−29.5445 kJ/mol) for CR, and (−18.8399 kJ/mol) for RR 120 indicated that the adsorption is exothermic during the adsorption of dyes onto the prepared kaolin adsorbent. Negative values of ΔS° (−0.141 kJ/mol) for BY 28, ΔS° (−0.096 kJ/mol) for CR and ΔS° (−0.072 kJ/mol) for RR 120 indicates that the randomness (disordered nature) at the solution-adsorbent interface decreased during the adsorption process of dyes onto kaolin adsorbent [62]. The disordered nature at the interface may be due to the higher translational entropy by the water molecule and with the loss of dyes uptaking.

Simultaneously, the magnitude of ΔH° and ΔG° indicates the adsorption process as physisorption (ΔG° , 0 to −20 kJ/mol and ΔH° , < 40 kJ/mol) and chemisorption (ΔG° , −80 to −400 kJ/mol and ΔH° , 40–120 kJ/mol) [63]. In this study, the values of ΔG° and ΔH° for BY 28, were favored the chemisorption process, and physisorption process for CR, and RR1 20 dyes.

3.5.3. Adsorption isotherms

An adsorption isotherm explains the mechanism of the sorption process which is the adsorbate (dyes) molecules interact with adsorbent and attain equilibrium. Most common and suitable adsorption isotherms are Langmuir and Freundlich [64]. Langmuir adsorption isotherm assumes that the adsorption occurs at specific homogenous sites and is the most suitable for monolayer adsorption, while the Freundlich adsorption isotherm model assumes that the formation of multilayer and heterogeneous systems due to non-uniform distribution of adsorption affinities and is not confined within the formation of monolayers [65].

The BY 28, CR, and RR120 dyes adsorption isotherms were

obtained using the linear form models Langmuir and Freundlich with governing equation presented in Eq. (10) and Eq. (11), respectively. Moreover, the essential characteristics of Langmuir isotherm can be also expressed in terms of their dimensionless equilibrium parameter, R_L as described in Eq. (12).

$$\frac{C_e}{q_e} = \frac{1}{K_L q_m} + \frac{C_e}{q_m} \quad (10)$$

$$\log q_e = \log K_F + \frac{\log C_e}{n} \quad (11)$$

$$R_L = \frac{1}{1 + K_L C_0} \quad (12)$$

where, C_e is the concentration of the dye solution (mg/L) at equilibrium, q_e is the amount of dye adsorbed on the adsorbent (mg/g) at equilibrium, K_L is the constant related to the free energy of adsorption (L/mg) and q_m is the monolayer adsorption capacity (mg/g).

The values of Langmuir isotherm constants q_m and K_L are obtained from the slope ($1/q_m$) and intercept ($1/K_L q_m$) of the straight-line plot of C_e/q_e versus C_e . R_L is a dimensionless equilibrium parameter, indicates the shape of the isotherm and the nature of the adsorption process ($R_L > 1$: unfavorable; $R_L = 1$: linear; $0 < R_L < 1$: favorable; $R_L = 0$: irreversible). K_F (mg/g) is a Freundlich constant (relative adsorption capacity of the adsorbent). n is a Freundlich constant that represents the adsorption intensity (strength). The value of n ranging from 1 to 10 indicated that the adsorption process is favorable. The values of K_F and n were calculated from the slope ($1/n$) and intercept ($\log K_F$) of the linear plot $\log q_e$ versus $\log C_e$.

The Langmuir isotherm is more favored for the uptake of BY 28, CR, and RR 120 dye onto prepared kaolin adsorbent having the correlation coefficient (R^2) value of 0.99713, 0.9991, and 0.998325, respectively. This indicates that adsorbents are monolayered that favored the chemical adsorption processes that take place. This is also confirmed with the pseudo-second-order kinetic model. The Langmuir and Freundlich isotherm plots are shown in Fig. 13 and Fig. 14, respectively with their corresponding correlation coefficient (R^2) with the calculated parameters (Table 4). The correlation coefficient (R^2) in the Langmuir isotherm model was relatively higher

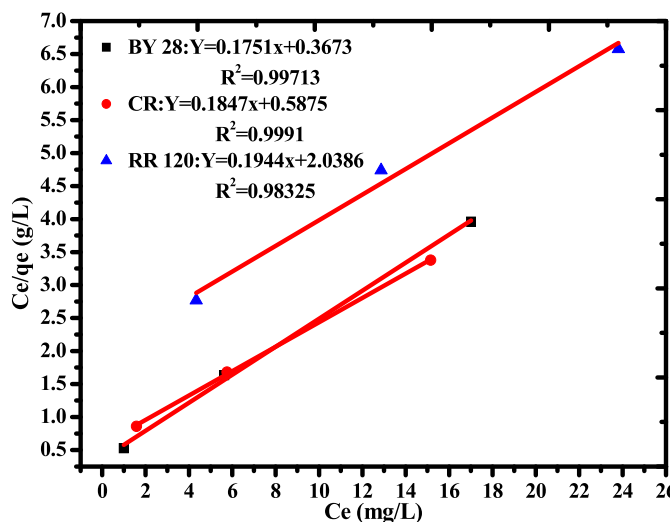


Fig. 13. Langmuir isotherm for BY28, CR, and RR120 onto kaolin adsorbent.

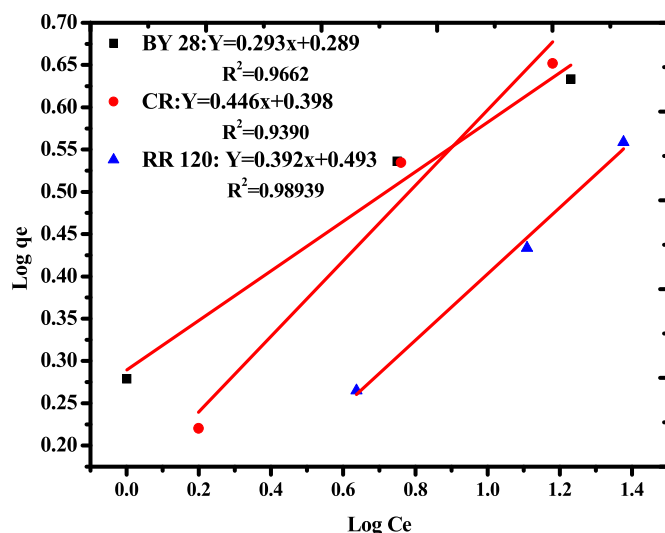


Fig. 14. Freundlich isotherm for BY28, CR, and RR120 onto kaolin adsorbent.

Table 4

Isotherm parameters for the adsorption of BY28, CR, and RR120 onto kaolin adsorbent.

Isotherm models	Parameters	Dyes		
		BY28	CR	RR120
Langmuir	R^2	0.99713	0.9991	0.998325
	q_m (mg/g)	5.71	5.41	1.09
Freundlich	K_L (L/mg)	0.578	0.315	0.454
	R^2	0.9662	0.9390	0.9894
	K_f (mg/g)	1.95	1.58	0.76
	n	3.46	2.51	2.03

(closer to unity) than the Freundlich isotherm model. This implied that the adsorption of BY 28, CR, and RR120 onto kaolin adsorbent is better described by the Langmuir isotherm model than the Freundlich isotherm model with the adsorption capacity of BY 28 = 5.71 mg/g, CR = 5.41 mg/g and RR 120 = 1.09 mg/g. These removal efficiencies and adsorption capacity differences may be attributed due to the unique chemical structure, physicochemical properties, and size (molecular weights) of the dye molecules [66]. In this work, the size of dye molecules in descending order are: BY 28 < CR < RR120 their corresponding adsorption capacity value of BY 28 > CR > RR 120 onto kaolin adsorbents which can be attributed due to their steric hindrance or crowdedness of the dyes molecules. Moreover, R_L values less than unity (Table 5), and n values greater than unity, revealed that the adsorption behavior of BY 28, CR, and RR 120 onto kaolin adsorbent was favorable (lie within the favorable limits) [67].

The removal efficiency of the presently studied dyes may be higher than previous reports and conversely may have low

Table 5

R_L (Dimensionless constant separation factor) values at different initial concentrations.

Dyes	R_L values		
	Concentration (mg/L)		
	20	40	60
BY28	0.079	0.041	0.028
CR	0.139	0.075	0.051
RR120	0.099	0.052	0.035

adsorption capacity with similar adsorbents. In this regard, the variation may be happened due to the solid-liquid (adsorbent amount to solution) ratio in the predetermined adsorption process. In addition to this, the number of active sites on the adsorbent and their surface area arises these controversies. Moreover, the tendency of dye molecule and/or ions in the solution to be loaded onto the prepared adsorbents ratio to that of stayed in solution. As described in the methodology section, used dyes are cationic and anionic in the solution that can be highly dependent on the ionic information, affinity, the hydration-free energy of dyes-kaolin adsorbent. The other important reason may be due to the volume of the solution and grams of the adsorbents. Furthermore, increasing the adsorption density onto the kaolin adsorbent may minimize further to adsorption of dyes by the adsorbates ion competition resulted in decreasing the void active sites on the surface of the adsorbent. Thus, in general, knowing the tenacity (whether the adsorption process is chemical or physical) of adsorbates binding onto the prepared adsorbents is critical for the evaluation of the maximum removal efficiency of each dye. As a result, it can be deduced the removal efficiency of the contaminants, in this study dyes, may not directly be related to the adsorption capacity which may result from the operating parameters, the adsorbents characteristics, and the solid-liquid interaction during the adsorption processes [68].

3.6. Removal efficiencies comparisons for BY 28, CR, and RR 120

The surface functional groups, the intensity of FTIR peaks of adsorbents (before adsorption of dyes), Adsorbent-BY 28, Adsorbent-CR, and Adsorbent-RR 120 before and after adsorption and adsorption results at each operational parameters were clearly explained that the adsorption mechanisms as shown in Fig. 15. According to adsorption results recorded, the percentage removal efficiency or adsorption capacity of BY 28, CR, and RR 120 dyes onto beneficiated kaolin adsorbent is probably caused by the molecular structure, molecular size, structure complexity of the type/nature of the dyes (cationic, and anionic) and with their basic, acidic, or reactive categories. The smaller molecular size, less crowded BY 28 probably may have better penetration into the internal pore structure of kaolin adsorbent and favored easier adsorption than higher molecular size dyes (CR and RR 120). For RR 120, with a larger molecular size, sterically hindered and minimal penetration into the internal pore structure of the adsorbents, and this partly explains why the removal efficiency of RR 120 is slightly poor and less efficient than that of BY 28 and CR. Hassani et al. (2014) reported a similar finding in that the molecular size and structural features of the adsorbates have a significant effect on the removal efficiency by certain adsorbents [69]. In addition, the mechanism of BY 28, CR, and RR 120 adsorption can be ascribed via electrostatic attractions between silanol (Si–OH) and aluminol (Al–OH) at the edges sites of the beneficiated kaolin adsorbent surfaces, as confirmed also with FTIR spectra, and the dyes molecules. Beneficiated kaolin has dominantly negatively charged surfaces during water activation, based on the high composition of silicon oxides [16], indicates BY 28 adsorption was high due to the electrostatic interaction of the cationic dye ($-N^+$) with the anionic groups (Si–O) that appeared on the kaolin surface. In the case of CR and RR 120, adsorption is due to the electrostatic interaction between the negatively charged sulfonate (SO_3^-) surface of the dye and the positively charged surface, aluminum oxides, of kaolin adsorbent (hydrated cations present in the interfoliar space) [42]. However, the dominant negatively charged surface of the beneficiated kaolin adsorbent (Si–O and Al–O) and CR (anionic, $2SO_3^-$) and RR 120 (highly anionic, $6SO_3^-$) were exhibited electrostatic repulsion which retards the adsorption process.

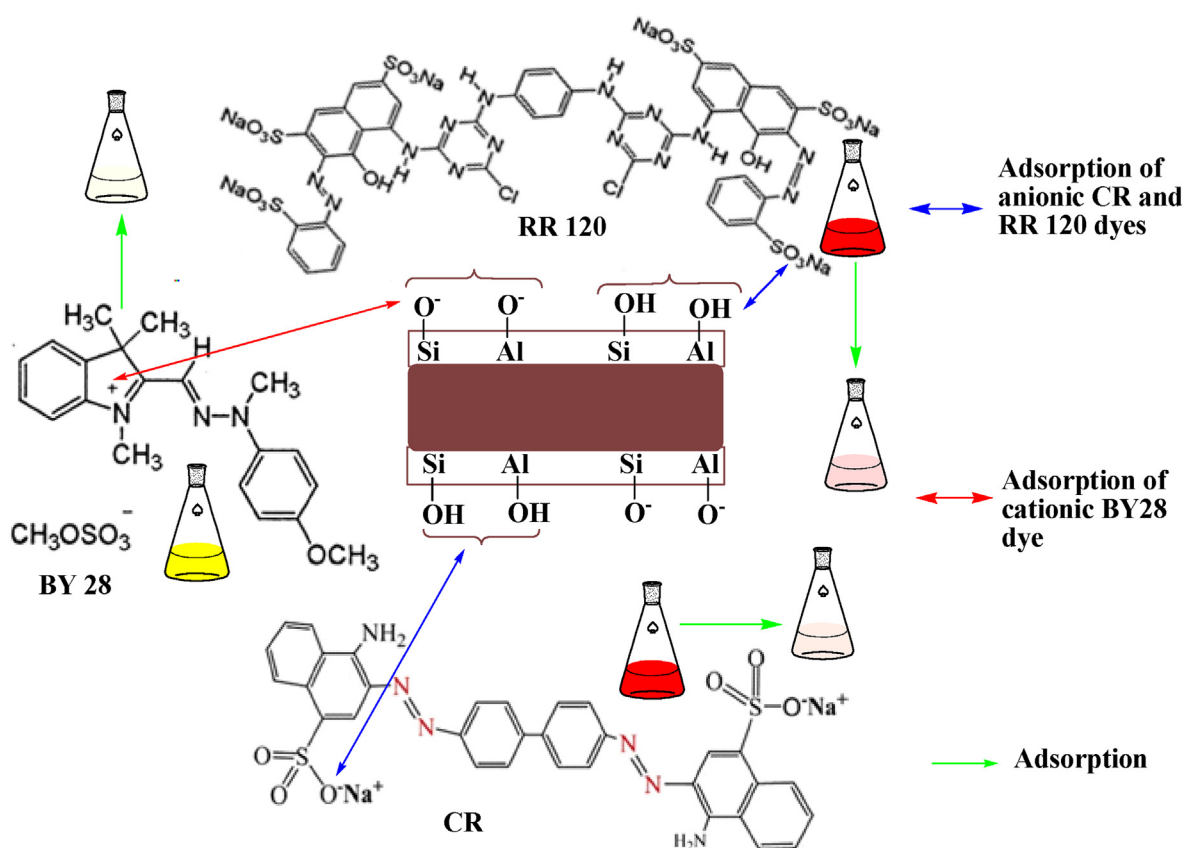


Fig. 15. Proposed adsorption mechanism (electrostatic interaction) of cationic (BY 28) and anionic (CR, RR 120) dyes onto kaolin adsorbents.

3.7. Comparison of dye adsorption capacity by the prepared adsorbents with some previous reports

The adsorption capacity of this study was compared with the effects of dyes onto kaolin adsorbent are shown in Table 6. As can be seen from Table 6, it was found varied adsorption capacities with varied experimental conditions. The dyes' adsorption capacity in the present study was varied with other kaolin adsorbents. In the comparison analysis, the adsorbent dosage, initial dye concentration, kinetic models, isotherms, and thermodynamics values and models were included. Moreover, dye types and classes used are varied. However, in the present study, three classes of dyes, each one from different classes were employed to evaluate the kaolin adsorbents capacity, hence it is critical compared with those dyes previously reported.

4. Conclusion

Natural clay minerals are recently attracting attention to be utilized as an alternative adsorbent contaminant purification in wastewater. The wet process was carried out for kaolin adsorbents preparation using Ethiopian kaolinite clay for the removal of three different modal dyes.

In this study, the adsorptive removal of BY 28, CR, and RR 120 dyes onto beneficiated kaolin adsorbents was evaluated. The adsorptive percentage removal efficiency of BY 28 (92.08%), CR (88.63%), and RR 120 (73.33%) were achieved with the prepared kaolin adsorbents under the optimum conditions of operating parameters, as adsorbent dosage = 1 g/100 mL, solution pH = 9 (for BY 28) and pH = 3 (for CR, RR 120), contact time = 60 min, initial dyes concentrations = 20 mg/L, and temperature = 30 °C. Based on

Table 6

Some previous studies comparison of adsorption capacities of dyes onto kaolin adsorbent.

Dyes	Dye class	Dosage	Dye con.	qmax (mg/g)	Isotherm	Kinetics	Thermodynamics	References
Crystal violet	Cationic	1 g/L	20 mg/L	47.3	L	PSO	$-\Delta G^\circ, -\Delta H^\circ, +\Delta S^\circ$	[33]
Brilliant green	Cationic	2 g/L	10 mg/L	65.42	L	PSO	$-\Delta G^\circ, -\Delta H^\circ, -\Delta S^\circ$	[70]
Methylene blue	Cationic	0.5 g/L	100 mg/L	52.76	L	PSO	$-\Delta G^\circ, +\Delta H^\circ, +\Delta S^\circ$	[10]
Basic Yellow 28	Cationic	2 g/L	10 mg/L	16.23	L	PSO	$-\Delta G^\circ, +\Delta H^\circ, +\Delta S^\circ$	[24]
Methylene Blue	Cationic	—	10 mg/L	29.85	L	PSO	$-\Delta G^\circ, +\Delta H^\circ, +\Delta S^\circ$	
Malachite Green	Cationic	—	10 mg/L	52.91	L	PSO	$-\Delta G^\circ, +\Delta H^\circ, +\Delta S^\circ$	
Acid green 25	Anionic	0.6 g/L	75 mg/L	23.26	L	PSO	—	[55]
Congo red	Anionic	100 g/L	150 mg/L	5.44	L	PSO	$-\Delta G^\circ, -\Delta H^\circ, -\Delta S^\circ$	[71]
Basic yellow 28	Cationic	10 g/L	20 mg/L	5.71	L	PSO	$-\Delta G^\circ, -\Delta H^\circ, -\Delta S^\circ$	This study
Congo red	Anionic	10 g/L	20 mg/L	5.41	L	PSO	$-\Delta G^\circ, -\Delta H^\circ, -\Delta S^\circ$	This study
Reactive red	Anionic	10 g/L	20 mg/L	1.09	L	PSO	$\Delta G^\circ, -\Delta H^\circ, +\Delta S^\circ$	This study

**L-Langmuir isotherm; PSO-Pseudo-Second-order.

the adsorption results, the adsorption process was mainly influenced by the molecular size through the effect of steric hindrance and surface charge upon the electrostatic interaction between the silanol (Si–OH) and aluminol (Al–OH) groups of kaolin and the surfaces of dyes. The dye BY 28 has a smaller molecular size and positively charged favored greater adsorption efficiency than CR and RR 120 due to the greater computation between the dye and kaolin adsorbent. While RR 120 has a bulk molecular size and is highly negatively charged shows the least percentage removal efficiency than BY 28 and CR due to minimal involvement between the dye and kaolin adsorbent. The adsorption rate and isotherm were better fitted by pseudo-second-order kinetics and Langmuir isotherm with $R^2 > 0.997$, which are close to unity. The thermodynamic study also indicates that the adsorption of dyes by kaolin is spontaneous and exothermic. Overall, we can conclude that all types of dyes, cationic (BY 28) and anionic (CR, RR 120) is removed by the prepared kaolin adsorbent from aqueous solutions and therefore is suitable for dye removal in wastewater treatment. However, it has been confirmed that the adsorbents from kaolin clay are highly dependent on the dye types and characteristics due to the surface charge nature of the kaolinite clay face that can make electrostatic interaction with ions of the dyes in the solution. Thus, we recommend an investigation through preliminary examination before utilizing the kaolinite clays as adsorbents for any type of dyes in the solution.

Author statement

Tadele Assefa Aragaw: Conceptualization, Project administration; Supervising, Writing - review & editing, Proofreading.

Adugna Nigatu Alene: Writing –First draft, Formal analysis, Graphics.

Funding

This work has not campaigned for any support.

Data availability

The data used to support the findings of this study are included in the article.

Ethical approval

This article does not contain any studies with animals performed by any of the authors.

Consent to participate

All authors participated in the research work underlying the content of the manuscript.

Consent to publish

All authors read and approved the final manuscript for submission.

Declaration of competing interest

The authors declare that they have no known competing financial interests or personal relationships that could have appeared to influence this work.

Declaration of competing interest

The authors declare that they have no competing interest.

Acknowledgment

The authors thank the Faculty of Chemical and Food Engineering, Bahir Dar Institute of Technology allowing us to use the laboratory materials, chemicals, and instruments. Also, we thank the faculty laboratory technicians.

References

- [1] P. Dhanke, A. Patil, V. Kore, P. Thakare, U. Patil, S. Wagh, Phosphate removal from industrial wastewater effluent using modified coal fly ash, *Desalination Water Treat.* 116 (2018) 232–241, <https://doi.org/10.5004/dwt.2018.22516>.
- [2] S. Zen, F.Z. El Berrichi, Adsorption of tannery anionic dyes by modified kaolin from aqueous solution, *Desalination Water Treat.* 57 (2016) 6024–6032, <https://doi.org/10.1080/19443994.2014.981218>.
- [3] D.S. Duc, N. Bin, T.T.H. Trang, Adsorption of basic yellow 28 in aqueous solution by activated carbon, *Asian J. Chem.* 25 (2013) 2173–2176, <https://doi.org/10.14233/ajchem.2013.13381>.
- [4] S. Liu, Q. Wang, H. Ma, P. Huang, J. Li, T. Kikuchi, Effect of micro-bubbles on coagulation flotation process of dyeing wastewater, *Separ. Purif. Technol.* 71 (2010) 337–346, <https://doi.org/10.1016/j.seppur.2009.12.021>.
- [5] G.L. Dotto, F.K. Rodrigues, E.H. Tanabe, R. Fröhlich, D.A. Bertuol, T.R. Martins, E.L. Foletto, Development of chitosan/bentonite hybrid composite to remove hazardous anionic and cationic dyes from colored effluents, *J. Environ. Chem. Eng.* 4 (2016) 3230–3239, <https://doi.org/10.1016/j.jece.2016.07.004>.
- [6] J. Georgin, G. Luiz, M. Antonio, E. Luiz, Journal of Environmental Chemical Engineering Preparation of activated carbon from peanut shell by conventional pyrolysis and microwave irradiation-pyrolysis to remove organic dyes from aqueous solutions, *Biochem. Pharmacol.* 4 (2016) 266–275, <https://doi.org/10.1016/j.jece.2015.11.018>.
- [7] S. Natarajan, H.C. Bajaj, R.J. Tayade, Recent advances based on the synergetic effect of adsorption for removal of dyes from waste water using photocatalytic process, *J. Environ. Sci. (China)* 65 (2018) 201–222, <https://doi.org/10.1016/j.jes.2017.03.011>.
- [8] T.A. Aragaw, F.M. Bogale, Biomass-based adsorbents for removal of dyes from wastewater: a review, *Front. Environ. Sci.* 9 (2021), 764958, <https://doi.org/10.3389/fenvs.2021.764958>.
- [9] P. Dhanke, A. Patil, V. Kore, N. Kanse, Phosphate removal from waste effluent using improved fly ash, *Mater. Today Proc.* 5 (2018) 17889–17894, <https://doi.org/10.1016/j.matpr.2018.06.116>.
- [10] L. Mouni, L. Belkhir, J.C. Bollinger, A. Bouzaza, A. Assadi, A. Tirri, F. Dahmoune, K. Madani, H. Remini, Removal of Methylene Blue from aqueous solutions by adsorption on Kaolin: kinetic and equilibrium studies, *Appl. Clay Sci.* 153 (2018) 38–45, <https://doi.org/10.1016/j.clay.2017.11.034>.
- [11] V. Vimonses, S. Lei, B. Jin, C.W.K. Chow, C. Saint, Adsorption of Congo red by three Australian kaolins, *Appl. Clay Sci.* 43 (2009) 465–472, <https://doi.org/10.1016/j.clay.2008.11.008>.
- [12] S. De Gisi, G. Lofrano, M. Grassi, M. Notarnicola, Characteristics and adsorption capacities of low-cost sorbents for wastewater treatment: a review, *SUSMAT* 9 (2016) 10–40, <https://doi.org/10.1016/j.susmat.2016.06.002>.
- [13] A. Iryani, D. Hartanto, Textile dyes removal by ZSM-5 from Bangka kaolin, in: *J. Phys. Conf. Ser.*, Institute of Physics Publishing, 2018, <https://doi.org/10.1088/1742-6596/1095/1/012011>.
- [14] S. Niu, X. Xie, Z. Wang, L. Zheng, F. Gao, Y. Miao, Enhanced removal performance for Congo red by coal-series kaolin with acid treatment, *Environ. Technol.* (2019) 1–25, <https://doi.org/10.1080/09593330.2019.1670269>, 0.
- [15] S. Bentahar, A. Dbik, M. El Khomri, N. El Messaoudi, A. Lacherai, Adsorption of methylene blue, crystal violet and Congo red from binary and ternary systems with natural clay: kinetic, isotherm, and thermodynamic, *J. Environ. Chem. Eng.* 5 (2017) 5921–5932, <https://doi.org/10.1016/j.jece.2017.11.003>.
- [16] T.A. Aragaw, F.T. Angerasa, Synthesis and characterization of Ethiopian kaolin for the removal of basic yellow (BY 28) dye from aqueous solution as a potential adsorbent, *Heliyon* 6 (2020), e04975, <https://doi.org/10.1016/j.heliyon.2020.e04975>.
- [17] O. Sözüdoğru, B.A. Fil, R. Boncukcuoğlu, E. Aladaş, S. Kul, Adsorptive removal of cationic (BY2) dye from aqueous solutions onto Turkish clay: isotherm, kinetic, and thermodynamic analysis, *Part. Sci. Technol.* 34 (2016) 103–111, <https://doi.org/10.1080/02726351.2015.1052121>.
- [18] E. Errais, J. Duplay, F. Darragi, I. M'Rabet, A. Aubert, F. Huber, G. Morvan, Efficient anionic dye adsorption on natural untreated clay: kinetic study and thermodynamic parameters, *Desalination* 275 (2011) 74–81, <https://doi.org/10.1016/j.desal.2011.02.031>.
- [19] E. Errais, J. Duplay, M. Elhabiri, M. Khodja, R. Ocampo, R. Baltenweck-Guyot, F. Darragi, Anionic RR120 dye adsorption onto raw clay: surface properties and adsorption mechanism, *Colloids Surfaces A Physicochem. Eng. Asp.* 403 (2012) 69–78, <https://doi.org/10.1016/j.colsurfa.2012.03.057>.
- [20] N. Abidi, J. Duplay, A. Jada, E. Errais, M. Ghazi, K. Semhi, M. Trabelsi-Ayadi,

- Removal of anionic dye from textile industries' effluents by using Tunisian clays as adsorbents. Zeta potential and streaming-induced potential measurements, *Compt. Rendus Chem.* 22 (2019) 113–125, <https://doi.org/10.1016/j.crci.2018.10.006>.
- [21] A.B. Karim, B. Mounir, M. Hachkar, M. Bakasse, A. Yaacoubi, Removal of Basic Red 46 dye from aqueous solution by adsorption onto Moroccan clay, *J. Hazard. Mater.* 168 (2009) 304–309, <https://doi.org/10.1016/j.jhazmat.2009.02.028>.
- [22] O. Yavuz, A.H. Aydin, Removal of direct dyes from aqueous solution using various adsorbents, *Pol. J. Environ. Stud.* 15 (2006) 155–161.
- [23] A. Boukhemkhem, K. Rida, Improvement adsorption capacity of methylene blue onto modified Tamazert kaolin, *Adsorpt. Sci. Technol.* 35 (2017), <https://doi.org/10.1177/0263617416684835>.
- [24] A.R. Tehrani-Bagha, H. Nikkar, N.M. Mahmoodi, M. Markazi, F.M. Menger, The sorption of cationic dyes onto kaolin: kinetic, isotherm and thermodynamic studies, *Desalination* 266 (2011) 274–280, <https://doi.org/10.1016/j.desal.2010.08.036>.
- [25] B.K. Nandi, A. Goswami, A.K. Das, B. Mondal, M.K. Purkait, Kinetic and equilibrium studies on the adsorption of crystal violet dye using Kaolin as an adsorbent, *Separ. Sci. Technol.* 43 (2008) 1382–1403, <https://doi.org/10.1080/01496390701885331>.
- [26] M. Dias, A. Valério, D. de Oliveira, A.A. Ulson de Souza, S.M.G.U. de Souza, Adsorption of natural annatto dye by kaolin: kinetic and equilibrium, *Environ. Technol.* (2019) 1–27, <https://doi.org/10.1080/09593330.2019.1578418>, 0.
- [27] J.E. Aguiar, J.A. Cecilia, P.A.S. Tavares, D.C.S. Azevedo, E.R. Castellón, S.M.P. Lucena, I.J. Silva, Adsorption study of reactive dyes onto porous clay heterostructures, *Appl. Clay Sci.* 135 (2017) 35–44, <https://doi.org/10.1016/j.clay.2016.09.001>.
- [28] T.R. Barbosa, E.L. Foletto, G.L. Dotto, S.L. Jahn, Preparation of mesoporous geopolymer using metakaolin and rice husk ash as synthesis precursors and its use as potential adsorbent to remove organic dye from aqueous solutions, *Ceram. Int.* 44 (2018) 416–423, <https://doi.org/10.1016/j.ceramint.2017.09.193>.
- [29] O.S. Ayanda, K.O. Sodeinde, P.O. Okolo, A.A. Ajayi, S.M. Nelana, E.B. Naidoo, Adsorptive behavior of kaolin for amido black dye in aqueous solution, *Orient. J. Chem.* 34 (2018) 1233–1239, <https://doi.org/10.13005/ojc/340305>.
- [30] A. Behnamfar, K. Chegni, R. Alaei, F. Veglio, The effect of thermal and acid treatment of kaolin on its ability for cyanide removal from aqueous solutions, *Environ. Earth Sci.* 78 (2019) 1–12, <https://doi.org/10.1007/s12665-019-8408-8>.
- [31] M. Gougazeh, F. Kooli, J.C. Buhl, Removal efficiency of basic blue 41 by three Zeolites prepared from natural Jordanian kaolin, *Clay Clay Miner.* 67 (2019) 143–153, <https://doi.org/10.1007/s42860-019-00016-1>.
- [32] P. Sejie, S. Nadiye-Tabbiruka, Removal of methyl Orange (MO) from water by adsorption onto modified Local clay (kaolinite), *Phys. Chem.* 6 (2016) 39–48, <https://doi.org/10.5923/j.pc.20160602.02>.
- [33] B.K. Nandi, A. Goswami, M.K. Purkait, Removal of cationic dyes from aqueous solutions by kaolin: kinetic and equilibrium studies, *Appl. Clay Sci.* 42 (2009) 583–590, <https://doi.org/10.1016/j.clay.2008.03.015>.
- [34] G.K. Sarma, S. Sen Gupta, K.G. Bhattacharyya, Removal of hazardous basic dyes from aqueous solution by adsorption onto kaolinite and acid-treated kaolinite: kinetics, isotherm and mechanistic study, *SN Appl. Sci.* 1 (2019) 1–15, <https://doi.org/10.1007/s42452-019-0216-y>.
- [35] T.A. Aragaw, F.T. Angerassa, Adsorption of basic yellow dye dataset using Ethiopian kaolin as an adsorbent, *Data Brief* 26 (2019), 104504, <https://doi.org/10.1016/j.dib.2019.104504>.
- [36] K.A. Abdulsalam, A.R.A. Giwa, J.M. Adelowo, Optimization studies for decolorization of textile wastewater using a sawdust-based adsorbent, *Chem. Data Collect.* 27 (2020), 100400, <https://doi.org/10.1016/j.cdc.2020.100400>.
- [37] L. Xia, S. Zhou, C. Zhang, Z. Fu, A. Wang, Q. Zhang, Y. Wang, X. Liu, X. Wang, W. Xu, Environment-friendly Juncus effusus-based adsorbent with a three-dimensional network structure for highly efficient removal of dyes from wastewater, *J. Clean. Prod.* 259 (2020), 120812, <https://doi.org/10.1016/j.jclepro.2020.120812>.
- [38] K. Litefti, M.S. Freire, M. Stitou, J. González-Álvarez, Adsorption of an anionic dye (Congo red) from aqueous solutions by pine bark, *Sci. Rep.* 9 (2019), 16530, <https://doi.org/10.1038/s41598-019-53046-z>.
- [39] T.A. Aragaw, Utilizations of electro-coagulated sludge from wastewater treatment plant data as an adsorbent for direct red 28 dye removal, *Data Brief* 28 (2020), 104848, <https://doi.org/10.1016/j.dib.2019.104848>.
- [40] E. Tiffo, A. Elimbi, J.D. Manga, A.B. Tchamba, Red ceramics produced from mixtures of kaolinite clay and waste glass, *Brazilian J. Sci. Technol.* 2 (2015), <https://doi.org/10.1186/s40552-015-0009-9>.
- [41] B. Lorentz, N. Shanahan, Y.P. Stetsko, A. Zayed, Characterization of Florida kaolin clays using multiple-technique approach, *Appl. Clay Sci.* 161 (2018) 326–333, <https://doi.org/10.1016/j.clay.2018.05.001>.
- [42] I. Chaari, E. Fakhfakh, M. Medhioub, F. Jamoussi, Comparative study on adsorption of cationic and anionic dyes by smectite rich natural clays, *J. Mol. Struct.* 1179 (2019) 672–677, <https://doi.org/10.1016/j.molstruc.2018.11.039>.
- [43] B. Davarcioglu, The Clay Minerals Observed in the Building Stones of Aksaray-Guzelyurt Area (Central Anatolia-Turkey) and Their Effects, 2010.
- [44] A. Kausar, M. Iqbal, A. Javed, K. Aftab, Z.I.H. Nazli, H.N. Bhatti, S. Nouren, Dyes adsorption using clay and modified clay: a review, *J. Mol. Liq.* 256 (2018) 395–407, <https://doi.org/10.1016/j.molliq.2018.02.034>.
- [45] T.C.N. Tan, T.K. Sen, Aqueous-phase methylene blue (MB) dye removal by mixture of eucalyptus bark (EB) biomass and kaolin clay (KC) adsorbents: kinetics, thermodynamics, and isotherm modeling, *Separ. Sci. Technol.* 55 (2020) 1036–1050, <https://doi.org/10.1080/01496395.2019.1580734>.
- [46] V.S. Munagapati, V. Yarramuthi, Y. Kim, K.M. Lee, D.S. Kim, Removal of anionic dyes (reactive black 5 and Congo red) from aqueous solutions using Banana peel powder as an adsorbent, *Ecotoxicol. Environ. Saf.* 148 (2018) 601–607, <https://doi.org/10.1016/j.ecoenv.2017.10.075>.
- [47] A.H. Jawad, A.S. Abdulhameed, Mesoporous Iraqi red kaolin clay as an efficient adsorbent for methylene blue dye: adsorption kinetic, isotherm and mechanism study, *Surface. Interfac.* 18 (2020), 100422, <https://doi.org/10.1016/j.surfin.2019.100422>.
- [48] M. Shaban, M.I. Sayed, M.G. Shahien, M.R. Abukhadra, Z.M. Ahmed, Adsorption behavior of inorganic- and organic-modified kaolinite for Congo red dye from water, kinetic modeling, and equilibrium studies, *J. Sol. Gel Sci. Technol.* 87 (2018) 427–441, <https://doi.org/10.1007/s10971-018-4719-6>.
- [49] K. Chinoune, K. Bentaleb, Z. Boubberka, A. Nadim, U. Maschke, Adsorption of reactive dyes from aqueous solution by dirty bentonite, *Appl. Clay Sci.* 123 (2016) 64–75, <https://doi.org/10.1016/j.clay.2016.01.006>.
- [50] R. Pleša Chicinaș, H. Bedeleian, R. Stefan, A. Maicăneanu, Ability of a montmorillonitic clay to interact with cationic and anionic dyes in aqueous solutions, *J. Mol. Struct.* 1154 (2018) 187–195, <https://doi.org/10.1016/j.molstruc.2017.10.038>.
- [51] B. Guo, J. Jiang, W. Serem, V.K. Sharma, X. Ma, Attachment of cerium oxide nanoparticles of different surface charges to kaolinite: molecular and atomic mechanisms, *Environ. Res.* 177 (2019) 108645, <https://doi.org/10.1016/j.envres.2019.108645>.
- [52] N.E.H. Fardjaoui, F.Z. El Berrichi, F. Ayari, Kaolin-issued zeolite A as efficient adsorbent for Bezanyl yellow and Nylomine green anionic dyes, *Microporous Mesoporous Mater.* 243 (2017) 91–101, <https://doi.org/10.1016/j.micromeso.2017.01.008>.
- [53] A.A. Adeyemo, I.O. Adeoye, O.S. Bello, Adsorption of dyes using different types of clay: a review, *Appl. Water Sci.* 7 (2017) 543–568, <https://doi.org/10.1007/s13201-015-0322-y>.
- [54] S. Mohebbi, D. Bastani, H. Shayesteh, Equilibrium, kinetic and thermodynamic studies of a low-cost biosorbent for the removal of Congo red dye: acid and CTAB-acid modified celery (Apium graveolens), *J. Mol. Struct.* 1176 (2019) 181–193, <https://doi.org/10.1016/j.molstruc.2018.08.068>.
- [55] P.S. Yap, V. Priyaa, Removal of crystal violet and acid green 25 from water using kaolin, *IOP Conf. Ser. Mater. Sci. Eng.* 495 (2019), <https://doi.org/10.1088/1757-899X/495/1/012052>.
- [56] P. Parthasarathy, S.K. Narayanan, Effect of hydrothermal carbonization reaction parameters on, *Environ. Prog. Sustain. Energy* 33 (2014) 676–680, <https://doi.org/10.1002/ep>.
- [57] T.A. Aragaw, Recovery of iron hydroxides from electro-coagulated sludge for adsorption removals of dye wastewater: adsorption capacity and adsorbent characteristics, *Surface. Interfac.* 18 (2020), 100439, <https://doi.org/10.1016/j.surfin.2020.100439>.
- [58] A.K. Kushwaha, N. Gupta, M.C. Chattopadhyaya, Removal of cationic methylene blue and malachite green dyes from aqueous solution by waste materials of Daucus carota, *J. Saudi Chem. Soc.* 18 (2014) 200–207, <https://doi.org/10.1016/j.jscs.2011.06.011>.
- [59] H. Zhu, X. Xiao, Z. Guo, X. Han, Y. Liang, Y. Zhang, C. Zhou, Adsorption of vanadium (V) on natural kaolinite and montmorillonite: characteristics and mechanism, *Appl. Clay Sci.* 161 (2018) 310–316, <https://doi.org/10.1016/j.clay.2018.04.035>.
- [60] A.N. Alene, G.Y. Abate, A.T. Habte, D.M. Getahun, Utilization of a Novel low-cost gibbo (Lupinus Albus) seed peel waste for the removal of malachite green dye: equilibrium, kinetic, and thermodynamic studies, *J. Chem.* (2021) 1–16, <https://doi.org/10.1155/2021/6618510>, 2021.
- [61] M. Asif Tahir, H.N. Bhatti, M. Iqbal, Solar Red and Brittle Blue direct dyes adsorption onto Eucalyptus angophoroides bark: equilibrium, kinetics and thermodynamic studies, *J. Environ. Chem. Eng.* 4 (2016) 2431–2439, <https://doi.org/10.1016/j.jece.2016.04.020>.
- [62] A. Oussalah, A. Boukerroui, A. Aichour, B. Djellouli, Cationic and anionic dyes removal by low-cost hybrid alginate/natural bentonite composite beads: adsorption and reusability studies, *Int. J. Biol. Macromol.* 124 (2019) 854–862, <https://doi.org/10.1016/j.ijbiomac.2018.11.197>.
- [63] W. Konicki, M. Aleksandrak, E. Mijowska, Equilibrium, kinetic and thermodynamic studies on adsorption of cationic dyes from aqueous solutions using graphene oxide, *Chem. Eng. Res. Des.* 123 (2017) 35–49, <https://doi.org/10.1016/j.cherd.2017.03.036>.
- [64] S.E. Subramani, N. Thinakaran, Isotherm, kinetic and thermodynamic studies on the adsorption behaviour of textile dyes onto chitosan, *Process Saf. Environ. Protect.* 106 (2017) 1–10, <https://doi.org/10.1016/j.psep.2016.11.024>.
- [65] Z. Huang, Y. Li, W. Chen, J. Shi, N. Zhang, X. Wang, Z. Li, L. Gao, Y. Zhang, Modified bentonite adsorption of organic pollutants of dye wastewater, *Mater. Chem. Phys.* 202 (2017) 266–276, <https://doi.org/10.1016/j.materchemphys.2017.09.028>.
- [66] G. Moussavi, M. Mahmoudi, Removal of azo and anthraquinone reactive dyes from industrial wastewaters using MgO nanoparticles, *J. Hazard. Mater.* 168 (2009) 806–812, <https://doi.org/10.1016/j.jhazmat.2009.02.097>.
- [67] A.A. Inyinbor, F.A. Adekola, G.A. Olatunji, Kinetics, isotherms and thermodynamic modeling of liquid phase adsorption of Rhodamine B dye onto Raphia hookeri fruit epicarp, *Water Resour. Ind.* 15 (2016) 14–27, <https://doi.org/10.1016/j.wri.2016.06.001>.

- [68] T.A. Aragaw, Recycling electro-coagulated sludge from textile wastewater treatment plants as an adsorbent for the adsorptions of fluoride in an aqueous solution, *Heliyon* 7 (2021), e07281, <https://doi.org/10.1016/j.heliyon.2021.e07281>.
- [69] A. Hassani, L. Alidokht, A.R. Khataee, S. Karaca, Optimization of comparative removal of two structurally different basic dyes using coal as a low-cost and available adsorbent, *J. Taiwan Inst. Chem. Eng.* 45 (2014) 1597–1607, <https://doi.org/10.1016/j.jtice.2013.10.014>.
- [70] B.K. Nandi, A. Goswami, M.K. Purkait, Adsorption characteristics of brilliant green dye on kaolin, *J. Hazard Mater.* (2009), <https://doi.org/10.1016/j.jhazmat.2008.03.110>.
- [71] V. Vimonses, S. Lei, B. Jin, C.W.K. Chow, C. Saint, Adsorption of Congo red by three Australian kaolins, *Appl. Clay Sci.* 43 (2009) 465–472, <https://doi.org/10.1016/j.clay.2008.11.008>.